HHS Public Access

Author manuscript

Structure. Author manuscript; available in PMC 2017 June 07.

Published in final edited form as:

Structure. 2016 June 7; 24(6): 897–905. doi:10.1016/j.str.2016.03.023.

The Structural Basis for Class II Cytokine Receptor Recognition by JAK1

Ryan Ferrao[1,3], **Heidi J.A. Wallweber**[1,3], **Hoangdung Ho**[1], **Christine Tam**[1], **Yvonne Franke**[1], **John Quinn**[2], and **Patrick J. Lupardus**[1,*]

[1]Departments of Structural Biology, Genentech, Inc., 1 DNA Way, South San Francisco, CA, 94080, USA

[2]Departments of Biochemical and Cellular Pharmacology, Genentech, Inc., 1 DNA Way, South San Francisco, CA, 94080, USA

SUMMARY

JAK1 is a member of the Janus kinase (JAK) family of non-receptor tyrosine kinases that are activated in response to cytokines and interferons. Here we present two crystal structures of the human JAK1 FERM and SH2 domains bound to peptides derived from the class II cytokine receptors IFN-λ receptor 1 and IL-10 receptor 1 (IFNLR1 and IL10RA). These structures reveal an interaction site in the JAK1 FERM that accommodates the so-called “box1” membrane-proximal receptor peptide motif. Biophysical analysis of the JAK1–IFNLR1 interaction indicates that the receptor box1 is the primary driver of the JAK1 interaction, and identifies residues conserved among class II receptors as important for binding. In addition, we demonstrate that a second “box2” receptor motif further stabilizes the JAK1–IFNLR1 complex. Together, these data identify a conserved JAK binding site for receptor peptides and elucidate the mechanism by which class II cytokine receptors interact with JAK1.

eTOC BLURB

The cytokine receptor box1 motif is critical for JAK kinase binding and activation. Ferrao et al. reveal the structure of box1 from class II cytokine receptors IFNLR1 and IL10RA bound to the FERM-SH2 domain of human JAK1, identifying a consensus motif for JAK1 interaction.

*To whom correspondence should be addressed. lupardus.patrick@gene.com (P.J.L.).

[3]These authors contributed equally to this work

AUTHOR CONTRIBUTIONS

R.F. and H.J.A.W performed protein purification. H.H. and H.J.A.W. conducted receptor interaction screen. C.T., and Y.F. generated constructs. H.J.A.W performed crystallization and optimization. R.F. and P.J.L. collected diffraction data, solved structures, and built molecular models. R.F. performed SEC-MALS and BLI. R.F. and J.Q. analyzed BLI data. P.J.L supervised the project. R.F., H.J.A.W, and P.J.L. wrote the manuscript.

ACCESSION NUMBERS

Coordinates and structure factors for JAK1 in complex with IFNLR1 and JAK1 in complex with the IFNLR1/IL10RA chimera have been deposited in the PDB under accession codes 5IXD and 5IXI.

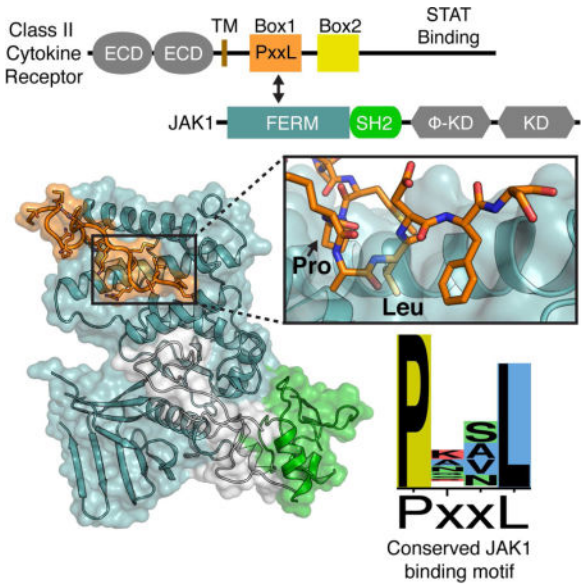

INTRODUCTION

Class I and class II cytokine receptors are responsible for recognition of cytokines and interferons in the extracellular environment and initiate intracellular signaling cascades that lead to an array of responses such as hematopoiesis, regulation of immune function, and cellular growth and development (Nicola and Hilton, 1998). Signaling through these two receptor families is dependent on the Janus kinases (JAKs), a family of multidomain non-receptor tyrosine kinases that are constitutively and non-covalently bound to their cognate signaling receptors (Leonard and O'Shea, 1998). The four JAK family members, JAK1, JAK2, JAK3, and TYK2 share a conserved domain organization consisting of N-terminal FERM and SH2 domains followed by a pseudokinase and kinase domain. The FERM and SH2 domains closely associate to form a FERM–SH2 "holodomain" required for binding to the cytoplasmic domain of cytokine receptors (Wallweber et al., 2014). Activity of the C-terminal kinase domain is essential for signaling, while the catalytically-impaired pseudokinase domain has been shown to play a regulatory role by suppressing kinase activity (Lupardus et al., 2014; Shan et al., 2014; Ungureanu et al., 2011). Ligand-mediated dimerization of two JAK-bound receptors facilitates kinase activation, leading to phosphorylation and nuclear translocation of STAT family transcription factors and transcription of target genes. Given their critical role in transducing cytokine signals, ablation of JAKs leads to severely compromised immune function (JAK3, TYK2) or embryonic (JAK2) or perinatal mortality (JAK1) (Casanova et al., 2012; Neubauer et al., 1998; Parganas et al., 1998; Rodig et al., 1998). In addition, mutant JAK alleles are associated with myeloproliferative neoplasms, hematologic cancers, and immune disorders (O'Shea et al., 2015). JAK1 in particular has pleiotropic effects on cytokine signaling, given its association with class I receptors of the common gamma and gp130 families as well as class II interferon receptors (Imada and Leonard, 2000).

Interferons (IFNs) are critical mediators of innate immunity against viral and bacterial infection in higher eukaryotes (Pestka et al., 2004). The IFN family can be classified into the Type I (IFN-α/β), Type II (IFN-γ), and Type III (IFN-λ) families, each with distinct roles in host pathogen responses (McNab et al., 2015; Schoenborn and Wilson, 2007; Wack et al., 2015). All IFNs, as well as the anti-inflammatory cytokine IL-10, signal through class II cytokine receptors, which dimerize in multiple combinations to generate distinct downstream outputs (Renauld, 2003). Among signaling pairs of class II receptors, one chain invariably has a long cytoplasmic domain, while its partner has a short cytoplasmic domain (Renauld, 2003). JAK1 is crucial for signaling through these class II receptor complexes, and associates with the receptor chains possessing long cytoplasmic domains (IFNGR1, IFNAR2, IFNLR1, IL10RA, IL22RA1, IL20RA).

Despite divergent sequence among class II receptors, the likelihood that they share a common ancestor (Renauld, 2003) suggests they may still bear a common sequence motif for JAK recognition. Twenty-five years ago, Murakami *et al*. described “box1” and “box2” sequences with this conserved character (Murakami et al., 1991) and subsequently box1 and box2 were shown to mediate the vital link between extracellular ligand-mediated dimerization and JAK activation (Haan et al., 2006). The box1 motif is a membrane proximal proline rich sequence, separated from the hydrophobic box2 motif by 10 to 40 residues. Mutations within the box1 and box2 motifs disrupt JAK binding as well as signaling (Haan et al., 2002; Lebrun et al., 1995; Murakami et al., 1991; Pelletier et al., 2006; Royer et al., 2005; Tanner et al., 1995; Usacheva et al., 2002; Yan et al., 1998), although sequence variability between receptors has made a unifying description of JAK-binding residues impossible. While the molecular basis of box2 recognition was recently described by the structure of IFN-α receptor 1 (IFNAR1) bound to the TYK2 FERM–SH2 (Wallweber et al., 2014), to date no structural information exists on how JAK FERM–SH2 domains recognize the box1 motif, nor have structures of other FERM–SH2 domains from the JAK family been described.

As the importance of juxtamembrane sequences in activation of receptor-mediated growth factor signaling systems has become clear (Endres et al., 2011; Haan et al., 2006), it seems likely that interplay between JAKs and their cognate cytokine receptors is critical to JAK activation. While much effort has been expended to identify the receptors and JAKs activated in response to many cytokines, a reductionist approach of systematically screening JAK/receptor interactions *in vitro* and validating these interactions using biophysical methods has not been performed. To begin this effort, we screened receptors known to signal through JAK1 for binding to the JAK1 FERM–SH2 *in vitro*, and used this information to guide the purification and crystallization of two class II cytokine receptors in complex with JAK1. These crystal structures and the accompanying mutational analysis identify the receptor box1 binding site in the FERM domain of JAK1 and elucidate a consensus box1 motif for class II cytokine receptors.

RESULTS

Characterization of receptor interactions with JAK1

To identify promising receptor candidates for co-crystallization with JAK1, we used an *in vitro* approach to assess interactions between JAK1 and cytokine receptors that signal through JAK1. First, we identified receptor cytoplasmic fragments containing putative box1 and box2 motifs by visual inspection of the primary sequences; in general, these sequences contained the first 40 to 60 residues C-terminal to the transmembrane domain (Figure S1). These human receptor sequences were cloned as GST-tagged fusion proteins and co-expressed with His-tagged human JAK1 FERM–SH2 (residues 35–559) in insect cells. To establish a direct interaction with JAK1, lysates from cells co-expressing GST-receptor and His-JAK1 constructs were subjected to a small scale Ni-IMAC pull-down assay to determine if the receptor co-purified with JAK1 (Figure 1A). Based on this screen, we identified a number of receptor fragments that both expressed well and interacted with JAK1. This included the class II cytokine receptors IFNAR2, IL10RA, IFNGR1, IFNLR1, and IL22RA1, and class I receptors from the common-γ (IL2RB, IL9R) and gp130 (IL6ST, OSMR, LEPR, and LIFR) families.

To confirm complex formation and further select the most suitable candidate for crystallography, His-JAK1/GST-receptor complexes were purified at large (>1L) scale, digested with TEV protease to release the His and GST tags, and subjected to size exclusion chromatography (SEC) to verify stable interaction. Using this methodology, we identified the class II cytokine receptor IFNLR1 (residues 250–299) complexed with the JAK1 FERM–SH2 as a strong candidate for structural studies (Figure 1B). To study the contributions of isolated IFNLR1 box1 and box2 sequences to JAK1 binding, we generated additional GST-tagged fragments of IFNLR1 containing putative box1 (residues 250–270) and box2 sequences (residues 270–299). Although co-purification with JAK1 was observed in the case of IFNLR1 box1 and box1/2 fragments, SEC analysis suggested that the IFNLR1 box1 peptide slowly dissociated from JAK1 during purification (Figure 1C). In contrast, the peptide containing IFNLR1 box1 and box2 was observed to form a stable complex with JAK1 (Figure 1C). The JAK1-IFNLR1 box1/box2 complex was judged to possess 1:1 stoichiometry when analyzed using Multi-Angle Light Scattering coupled to size exclusion chromatography (SEC-MALS) (Figure S2). Interestingly, the box2 fragment of IFNLR1 did not co-purify with JAK1 (Figure 1C).

To quantify the interaction between JAK1 and IFNLR1, we performed BioLayer Interferometry (BLI) with immobilized IFNLR1 peptides incubated with increasing concentrations of JAK1 FERM–SH2 (Figures 1D and S2). Based on kinetic analysis using a 1:1 binding model (see Supplemental Methods), the effective dissociation constant between JAK1 FERM–SH2 and IFNLR1 box1/box2 (residues 250–299) was determined to be 70.5 ± 0.2 nM (Figure 1D and Table 1). Measured individually, the IFNLR1 box1 motif (residues 250–270) bound JAK1 with a dissociation constant of 1.23 ± 0.01 μM (Table 1 and Figure S2), while an IFNLR1 box2 containing peptide (residues 270–299) showed no detectable binding to JAK1 (Figure S2). Given that the association rate constants were similar for JAK1 binding to IFNLR1 box1/box2 (residues 250–299) and IFNLR1 box1 (residues 250–270) we

suggest that the 17-fold increase in binding potency can be attributed to an increase in complex stability which results from the presumably hydrophobic JAK1-box2 interaction. To confirm the contribution of the predicted box2 located at residues 290–293, we performed BLI on an IFNLR1 peptide truncated immediately preceding this motif (box1Δbox2, residues 250–289) (Table 1 and Figure S2). Removal of this box2 motif significantly reduced binding affinity, with a dissociation constant of 1.57 ± 0.01 μM. Overall, this analysis indicates that the box1 site is the primary JAK1–IFNLR1 binding site, while box2 stabilizes the interaction. This result is in significant contrast to TYK2 interaction with IFNAR1, which required the box2 fragment for stability *in vitro* (Wallweber et al., 2014).

The structure of the JAK1 FERM–SH2 in complex with IFNLR1

To structurally elucidate the interaction between JAK1 and IFNLR1, we co-expressed human JAK1 FERM–SH2 (residues 35–559) with the GST-tagged IFNLR1 box1/box2 fragment (residues 250–299) for crystallization. These efforts yielded a 2.85Å dataset that was solved by molecular replacement using the FERM domain of TYK2 (Table 2). The FERM–SH2 module of JAK1 shares the same overall architecture with that of TYK2 (Wallweber et al., 2014), consisting of four sub-domains packed into a Y-shaped receptor interaction domain (Figure 2A). These sub-domains include an N-terminal ubiquitin-like F1 (residues 36–111), an acyl-CoA binding protein-like F2 (residues 148–282), a pleckstrin homology-like F3 (residues 283–419), and a SH2 domain (residues 440–526). The F1, F2, and F3 subdomains closely associate into a canonical tri-lobed FERM domain, with the SH2-like domain packed against the F1 and F3 domains forming the base of the “Y”. The JAK1 SH2 domain is moderately disordered in the structure, and only an incomplete model could be built into the electron density. Like TYK2, the F2 domain of JAK1 contains a large basic patch that suggests close proximity to the plasma membrane *in vivo* (Figure S3).

After JAK1 model refinement, additional electron density was visible next to the FERM F2 sub-domain, in proximity to a groove lined by the α2, α3, and α4 helices (Figure S4). To aid in the correct placement of the IFNLR1 peptide, which contains methionines at positions 253 and 263, we reproduced the JAK1–IFNLR1 crystals labeled with selenomethionine and collected a dataset at the Selenium K-edge (Table 2). Signal corresponding to the two selenomethionine residues in the labeled IFNLR1 peptide allowed us obtain the peptide register and unambiguously model 21 residues of IFNLR1, including the box1 motif, into this density (Figures 2B and S4). The first visible residue, K250, is the first intracellular residue immediately following the transmembrane helix (Figure 2B). The interaction between IFNLR1 and JAK1 buries approximately 2060 $Å^2$ of surface area and can be broken down into two separate contact interfaces (Figure 2B). The first interface is mediated by IFNLR1 residues 252 to 259 (LMGNPWFQ), beginning with a backbone contact between IFNLR1 Leu252 and the JAK1 Asn233 sidechain and culminating with a short 3_{10} helix that inserts Trp257 into a pocket formed by JAK1 residues Glu186, His183, and Leu190 of helix F2-α2, and residues Ile240 and Val243 of helix F2-α3 (Figure 2C). JAK1 Glu186 forms the base of this pocket, forming a hydrogen bond with the indole nitrogen of Trp257. Additional contacts at this site include hydrogen bonds between JAK1 Arg239 and the mainchain

carbonyls of IFNLR Trp257 and Gln259 and between the sidechains of JAK1 Gln180 and IFNLR1 Gln259.

Following Gln259, the IFNLR1 peptide backbone bulges away from JAK1, coming back into contact again at Met263 (Figure 2D). This section of the IFNLR1 binding interface is mediated by a second short 3_{10} helix between residues Pro264 and Leu267. This helix aligns the sidechains of Pro264, Leu267, and Phe269, forming a hydrophobic ridge that fills a hydrophobic pocket lined by JAK1 residues Phe247 and Phe251 of helix F2-α3, Val194 and Leu195 of helix F2-α2, Val261 of the F2-α3/α4 linker, and Leu266 of helix F2-α4. Additional polar contacts are made between the backbone amide nitrogens of IFNLR1 Arg265 and Ala266 and JAK1 Glu188, the sidechains of IFNLR1 Arg265 and JAK1 Asp184, and IFNLR1 Asp268 carbonyl oxygen and JAK1 Lys269. Beyond Ser270, the electron density for IFNLR1 is poor, suggesting disorder of the peptide backbone likely due to a lack of contacts with JAK1. In addition, we were unable to model the IFNLR1 box2 motif due to significant structural disorder in the JAK1 SH2 domain.

To identify IFNLR1 residues critical for the interaction with JAK1, we generated several IFNLR1 box1 peptides (residues 250–270) containing alanine substitutions predicted to abrogate binding and measured their affinity for the JAK1 FERM–SH2 by BioLayer Interferometry (Figures 3A and S2). The IFNLR1 PWF motif was of particular interest, given the deep insertion of Trp257 into the pocket formed by the F2 α2 and α3 helices. Surprisingly, we found mutation of Trp257 to alanine only slightly decreased the affinity of IFNLR1 for JAK1. In contrast, individual alanine substitution of residues Pro264, Leu267, or Phe269, which form the JAK1-facing side of the short 3_{10} helical PRALDF motif, resulted in a near abrogation of IFNLR1 binding. Lastly, mutagenesis of IFNLR1 residues Arg260, Lys262 and Arg265, which have side chains that point away from JAK1, had only a minimal effect on the interaction. These studies indicate that the PxxLxF motif contributes the bulk of the binding energetics to the interaction between IFNLR1 and JAK1.

To validate the peptide binding site on JAK1, we made substitutions in several JAK1 residues shown to contact IFNLR1 and tested the ability of these mutants to bind the wild-type IFNLR1 box1 peptide (Figure 3B). As expected on the basis of receptor alanine mutations, change of JAK1 residue Ile240 to either leucine or phenylalanine, which would be expected to sterically block IFNLR1 Trp257 insertion, had only a minor effect on the affinity of the interaction. Conversely, mutation of the JAK1 Glu188 sidechain, which interacts with the backbone amide nitrogens from IFNLR1 Arg265 and Ala266, to alanine resulted in a large drop in IFNLR1 affinity. Additionally, mutation of Gly191 to leucine, which would be expected to sterically block IFNLR1 Leu267, also disrupted the interaction between JAK1 and IFNLR1. These results validate the JAK1 FERM F2 subdomain as the interaction site for the IFNLR1 box1 motif.

Structure of JAK1 bound to an IFNLR1/IL10RA chimeric receptor

To ascertain whether the interaction of IFNLR1 with JAK1 is emblematic of the class II cytokine receptor family, we attempted crystallization of a second JAK1/class II receptor complex. IL10RA was identified as a strong JAK1 binder in our pull down analysis (Figure 1A) and formed a stable complex with JAK1 (Figure S5). Surprisingly, we were unable to

grow crystals of this complex, despite high homology between the key JAK1 binding motif in IFNLR1 and a similar motif in IL10RA (PRALDF vs. PSVLLF). In an attempt to understand this lack of crystal formation, we analyzed the JAK–IFNLR1 crystal lattice and discovered that a unique N-terminal IFNLR1 peptide motif formed an extensive crystal contact with the F3 subdomain of a neighboring JAK1 FERM domain (Figure S5). To take advantage of this contact, we designed a chimeric receptor containing the crystal contact residues as well as Trp257 from IFNLR1 (residues 250–260) fused N-terminal to a fragment of IL10RA (residues 264–303), which contains the IL10RA box1 PSVLLF motif and box2 residues, and prepared this receptor–JAK1 complex for crystallography. We obtained crystals of JAK1 in complex with this IFNLR1–IL10RA chimeric receptor that yielded a 2.56Å dataset (Table 2). Unexpectedly, this complex crystallized in a different spacegroup ($C222_1$ for IFNLR1 versus C2 for the chimeric receptor) yet preserved the crystal contact between the peptide and the JAK1 F3 subdomain of a neighboring molecule (Figure S5). The structure was solved by molecular replacement using the JAK1 FERM–SH2 model, and the higher resolution allowed for the building of additional residues in the SH2 domain, as well as 29 residues from the chimeric receptor peptide (Figure S5). Importantly, this peptide binds to the α2/α3 peptide binding groove on the surface of the JAK1 FERM F2 subdomain in a similar conformation to wild-type IFNLR1 (Figure 4A). In the chimeric receptor structure, the IFNLR1 PWF motif as well as the Pro, Leu, and Phe residues from the IL10RA PSVLLF motif adopt a near identical conformation to that seen for wild type IFNLR1 (backbone rmsd 0.62 Å for IFNLR1 residues 263–269 compared to IL10RA residues 266–272) (Figure 4B). These data strongly suggest that the PxxLxF motif found in IFNLR1 and IL10RA is a conserved JAK1-interaction motif.

In addition to the interaction between the chimeric receptor and the JAK1 FERM F2 subdomain, the electron density for the peptide extends away from the FERM domain and approaches the SH2 domain of a crystallographically-related JAK molecule in the lattice (Figure 4C). IL10RA residues 278–281 bind to the SH2 box2 peptide groove of this neighboring JAK1 molecule, forming a short two-strand parallel sheet with the SH2 βG1 strand in a reversed direction when compared to the interaction of IFNAR1 with the TYK2 SH2 domain (Wallweber et al., 2014)(Figures 4D and S5). Given the reversed direction of this peptide sequence and location outside of the conventional box2 position, we cannot rule out the possibility that this interaction is formed only under crystallization conditions. Yet this unique interaction raises interesting questions about the promiscuity of the box2 binding site (discussed below).

A JAK1 binding motif is conserved in Class II cytokine receptors

Class II cytokine receptors, which are responsible for signaling through interferons and IL-10 family cytokines, are characterized by two subtypes (Renauld, 2003). One subtype has a short intracellular domain (<100 residues) that typically interacts with either JAK2 or TYK2. The second subtype has a longer intracellular domain (>200 residues) that interacts with JAK1. Given that the PxxLxF motif is highly conserved among orthologs of the class II receptors IFNLR1 and IL10RA (Figure S6), we compared the juxtamembrane sequences for all six human class II cytokine receptors with long intracellular domains (i.e. JAK1-associated class II receptors). Multiple sequence alignment shows that all six long chain

class II receptors share a proline followed by a leucine two residues downstream (Figure 5A). The Phe residue is also conserved in IFNAR2, but varies in IL20RA, IL22RA1, and IFNGR1 (Leu, Val, and Ser respectively). A logo plot of orthologs of the JAK1-interacting class II receptors shows universal conservation of the PxxL motif among higher eukaryotes (Figure 5B). This conserved box1 binding motif likely provides the specificity required for JAK1 recruitment and subsequent kinase activation and signaling in class II receptors.

DISCUSSION

The box1 cytokine receptor motif is indispensable for both JAK binding, kinase signaling, and downstream STAT activation (Haan et al., 2006). Despite its critical importance, representative structural information on the box1 interaction with JAKs has been lacking. In addition, uncertainty about how the box1 motif binds has been amplified by the lack of sequence conservation between receptor paralogs that bind the same JAK. The JAK1–IFNLR1 and JAK1–IL10RA structures presented here now allow us to decipher a “code” by which JAK1 interacts with the class II family of receptors. Our structural and biophysical analysis indicate that a conserved PxxLxF motif is essential for IFNLR1 binding, and a structure of IL10RA strongly suggests this receptor has the same requirements. Importantly, published work has shown that residues within the PxxLxF motif are necessary for the interaction between IL10RA and JAK1 (Usacheva et al., 2002), and this segment was found to be essential for JAK1 binding and signaling through IFNGR1 (Usacheva et al., 2002). Supporting the importance of the box1 PxxLxF motif, several other receptors from the common-γ family (IL-2Rβ, IL-9R, and IL-21R) contain a related box1 PxPxxF motif (Goldsmith et al., 1994; Zhu et al., 1998).

On the other hand, we found that several weakly conserved IFNLR1 contact residues between the transmembrane domain and the PxxLxF motif were dispensable for JAK1 binding. In particular, Trp257, which is buried in a pocket between the α2 and α3 helices in the FERM F2 subdomain showed only a 3-fold reduction in binding from wild type when mutated to alanine. Interestingly, juxtamembrane tryptophan residues in both gp130 (JAK1 binder) and EPOR (JAK2 binder) have been implicated in signaling, but not JAK binding (Constantinescu et al., 2001; Haan et al., 2002). While it may follow that IFNLR1 Trp257 has a role in activation of an IFNλ-stimulated signaling complex, tryptophan residues are not universally conserved in receptor sequences near the membrane. IL10RA, for example, has a short juxtamembrane sequence upstream of the box1 motif consisting of three Arg residues followed by two Lys residues, suggesting that the box1 motif is sufficient for binding and signaling through IL10RA and IL10RB.

Our characterization of JAK1 and IFNLR1 indicates that box1 is the primary driver of the JAK1-IFNLR1 interaction, and to our knowledge this represents the first *in vitro* biophysical dissection of the individual contributions of box1 and box2 residues to a receptor-JAK interaction. Importantly, the IFNLR1 box2 has very poor affinity for JAK1 by itself; however, addition of box2 to the box1 sequence drives a 17-fold increase in affinity. Based on kinetic analysis, this affinity increase is driven primarily by a decreased off-rate for the peptide containing box1 and box2. A structure of TYK2 in complex with IFNAR1 previously revealed that box2 binds in a cleft in the SH2 domain forming a short antiparallel

β-sheet interaction (Wallweber et al., 2014). Alignment of the JAK1–IFNLR1 structure presented here with this TYK2–IFNAR1 structure (PDB code 4PO6) shows that the C-terminus of IFNLR1 bound to JAK1 lines up with the N-terminus of IFNAR1 bound to TYK2 (Figure 6). This compatible topology indicates that simultaneous binding of box1 and box2 to a single JAK monomer is possible, providing a rationale for the box2-driven increase in receptor binding potency we observe. We speculate that the hydrophobic box2 interaction may exhibit slow association/dissociation kinetics, where occupancy is achieved very slowly in the absence of the box1 interaction. This hypothesis is consistent with our inability to isolate a stable JAK1–IFNLR1 box2 complex in solution (Figure 1C). However, the stabilizing effect that box2 confers in the context of a full receptor peptide is dramatic, owing to its relatively slow dissociation kinetics.

Yet despite this biophysical evidence and the topologic potential for both receptor box1 and box2 motifs binding to a single JAK1 molecule, in our structures of JAK1 with IFNLR1 and the IFNLR1–IL10RA chimera (which contains the IL10RA box1 and box2) we do not observe an intermolecular 1:1 interactions between receptor and JAK1. Instead, for IL10RA we see a crossover interaction with a hydrophobic “box2-like” motif interacting with a neighboring JAK1 SH2 domain within the lattice (Figure 4C), while for IFNLR1, the box2 along with much of the SH2 domain is disordered. At this moment we have no evidence that either of these box2-unbound conformations are physiological, but the absence of box2 binding in structures for two separate receptors with relatively diverse sequence raises an interesting question about crossover interactions between a single receptor and two JAKs *in vivo*. While speculative, the crossover of box2 to a second, different JAK molecule could represent a distinct active or inactive signaling conformation, in particular for heterodimeric signaling receptor complexes that utilize two different types of JAKs (i.e. JAK1 and TYK2).

On the JAK side of the interaction, conservation analysis of the box1 binding groove indicates this region is highly conserved among JAKs in general (McNally and Eck, 2014), suggesting involvement of this interface in receptor binding among the other JAK isoforms. Intriguingly, we find the box1 interaction between IFNLR1 and JAK1 to be distinct from the FERM F3 subdomain peptide interaction sites identified in structures of FERM-containing adapter proteins bound to intracellular domains from a number of cell adhesion molecules (Anthis et al., 2009; Hamada et al., 2000; Li et al., 2014; Wei et al., 2015). Instead, the box1 site is similar to a region engaged by autoinhibitory peptides that bind FERM domains from two ERM family proteins Moesin and Merlin (Li et al., 2015; Pearson et al., 2000) (Figure S7). Our structures of the JAK1 FERM–SH2 show that the α2-α3 helices of the FERM F2 subdomain are extended (α2 and α3 helices extended by three and two turns, respectively) when compared to the ERM proteins or the FERM domain of Focal Adhesion Kinase (Ceccarelli et al., 2005; Hamada et al., 2000; Pearson et al., 2000), suggesting co-evolution of the JAK FERM F2 binding site along with receptor intracellular domains to create the specificity and affinity required for properly tuned cytokine signaling. Given high receptor sequence diversity and the presence of multiple receptor binding site on the JAKs, it appears likely that resulting differences in structure and affinity between JAKs and bound receptors ultimately affects signaling outputs of these key receptor/kinase signaling systems.

EXPERIMENTAL PROCEDURES

Cytokine Receptor Interaction Screen

Fragments of human cytokine receptors predicted to contain the box1 and box2 binding sites were cloned into a pAcGP67-based vector with a N-terminal GST tag and a TEV cleavage site. Human JAK1 FERM-SH2 (G35-K559) was also cloned into a pAcGP67-based vector with an N-terminal His6 tag and a TEV cleavage site. Sf9 cells we infected with the resulting receptor-GST and His-JAK1 baculovirus, and after 72 hours cells were lysed by sonication, and lysates subjected to Ni-IMAC pull-down assay as described in Supplemental Information. Eluates were then subjected to SDS-PAGE and visualized with the Criterion Stain Free Imager (BioRad).

Protein Expression and Purification

For preparation of the JAK1/IFNLR1 complex for crystallization, His-JAK1 FERM-SH2 (G35-K559) and GST-IFNLR1 (K250-T299) constructs as described above were used for large-scale protein expression. For the JAK1 complex with the IFNLR1/IL10RA chimera, a DNA fragment containing codons for IFNLR residues K250-R260 followed by IL-10RA residues K264-K303 was synthesized and cloned into the pAcGP67 GST-TEV vector. JAK1–IFNLR1 and JAK1–IFNLR1/IL10RA complexes were produced by co-infection at a 1:1 viral ratio. Harvested cells were lysed and purified by Ni-IMAC followed by SEC. Fractions containing complex were cleaved with TEV, subjected to a second round of SEC, and concentrated for crystallization as detailed in Supplemental Information.

Crystallization and Data Collection of JAK1-IFNLR1 and JAK1-IL10RA

Native and Seleneomethionine-derivatized crystals of JAK1-IFNLR1 were grown in hanging drops by vapor diffusion at 4 °C with mother liquor containing 0.1–0.2 M Ammonium citrate tribasic pH 7 and 5–15% PEG 3350. Streak seeding and dehydration were necessary to obtain diffraction quality crystals. Crystals of JAK1–IFNLR1/IL10RA were grown in hanging drops by vapor diffusion with mother liquor containing 0.1 M MES pH 6.5, 0.2 M $MgCl_2$, 10% PEG 4000, 10% Ethylene Glycol, and Sodium Malonate pH 7.0. Streak seeding was necessary to obtain diffraction quality crystals. Crystals were cryoprotected and preserved for data collection by swift immersion in liquid N2. Data was collected at 100K at beamline 12-2 of the Stanford Synchrotron Radiation Lightsource and beamline 5.0.2 at the Advanced Light Source and processed with XDS and XSCALE.

Structure Determination

The structure of JAK1–IFNLR1 was determined by molecular replacement using the FERM domain of TYK2 (PDB ID 4PO6) as a search model. The structure of JAK1–IFNLR1/IL10RA chimera was solved by molecular replacement using a search model derived from the JAK1–IFNLR1 structure. The final JAK1–IFNLR1 model was refined at 2.85 Å to a R/Rfree of 24.9/28.2%. The final JAK1–IFNLR1/IL10RA model was refined at 2.57 Å to a R/Rfree of 21.3/25.5%. Full details on structure solution, model building, and refinement can be found in Supplemental Information. All residues in the final chimeric peptide are labeled based on the IL10RA numbering scheme.

BioLayer Interferometry

The BioLayer Interferometry (BLI) assay was performed in triplicate on an Octet RED384. Synthetic peptides were immobilized on streptavidin biosensors, and the association and dissociation of JAK1 FERM-SH2 with IFNLR1 Box1/Box2 was measured. Curves were double referenced and averaged, followed by global fitting to a 1:1 kinetic interaction model as described in Supplemental Information. To analyze the effect that IFNLR1 and JAK1 mutations have on the affinity of the IFNLR1-JAK1 interaction, BLI data of IFNLR1 and JAK1 variants were analyzed using a steady-state affinity model. The response of double referenced and averaged data at equilibrium was plotted as a function of concentration and fit with a 1:1 binding model. R_{max} was constrained to global values.

Sequence Alignment and Sequence Logo Plot

Sequence alignment figures were generated using T-Coffee. For sequence logos, class II cytokine receptor box1 sequences from a variety of species were aligned and generated using Weblogo 3. Receptors used for alignment and analysis are available in Supplemental Information.

Supplementary Material

Refer to Web version on PubMed Central for supplementary material.

Acknowledgments

We thank H. Maun, H. Kaluarachchi, A. Estevez, K. Bai, J. Sampang, K. Mortara, and the Biomolecular Engineering group at Genentech for their technical assistance, and E. Dueber for critical reading of the manuscript. The Advanced Light Source is supported by the Director, Office of Science, Office of Basic Energy Sciences, of the U.S. Department of Energy under Contract No. DE-AC02-05CH11231. Use of the Stanford Synchrotron Radiation Lightsource, SLAC National Accelerator Laboratory, is supported by the U.S. Department of Energy, Office of Science, Office of Basic Energy Sciences under Contract No. DE-AC02-76SF00515. The SSRL Structural Molecular Biology Program is supported by the DOE Office of Biological and Environmental Research, and by the National Institutes of Health, National Institute of General Medical Sciences (including P41GM103393). The contents of this publication are solely the responsibility of the authors and do not necessarily represent the official views of NIGMS or NIH.

References

Anthis NJ, Wegener KL, Ye F, Kim C, Goult BT, Lowe ED, Vakonakis I, Bate N, Critchley DR, Ginsberg MH, Campbell ID. The structure of an integrin/talin complex reveals the basis of inside-out signal transduction. EMBO J. 2009; 28:3623–3632. DOI: 10.1038/emboj.2009.287 [PubMed: 19798053]

Casanova JL, Holland SM, Notarangelo LD. Inborn Errors of Human JAKs and STATs. Immunity. 2012; 36:515–528. DOI: 10.1016/j.immuni.2012.03.016 [PubMed: 22520845]

Ceccarelli DFJ, Ceccarelli DFJ, Song HK, Song HK, Poy F, Poy F, Schaller MD, Schaller MD, Eck MJ, Eck MJ. Crystal Structure of the FERM Domain of Focal Adhesion Kinase. J Biol Chem. 2005; 281:252–259. DOI: 10.1074/jbc.M509188200 [PubMed: 16221668]

Constantinescu SN, Huang LJ, Nam H, Lodish HF. The erythropoietin receptor cytosolic juxtamembrane domain contains an essential, precisely oriented, hydrophobic motif. Molecular Cell. 2001; 7:377–385. [PubMed: 11239466]

Endres NF, Engel K, Das R, Kovacs E, Kuriyan J. Regulation of the catalytic activity of the EGF receptor. Current Opinion in Structural Biology. 2011; 21:777–784. DOI: 10.1016/j.sbi.2011.07.007 [PubMed: 21868214]

Goldsmith MA, Xu W, Amaral MC, Kuczek ES, Greene WC. The cytoplasmic domain of the interleukin-2 receptor beta chain contains both unique and functionally redundant signal transduction elements. J Biol Chem. 1994; 269:14698–14704. [PubMed: 8182077]

Haan C, Heinrich PC, Behrmann I. Structural requirements of the interleukin-6 signal transducer gp130 for its interaction with Janus kinase 1: the receptor is crucial for kinase activation. The Biochemical journal. 2002; 361:105–111. [PubMed: 11742534]

Haan C, Kreis S, Margue C, Behrmann I. Jaks and cytokine receptors—An intimate relationship. Biochemical Pharmacology. 2006; 72:1538–1546. DOI: 10.1016/j.bcp.2006.04.013 [PubMed: 16750817]

Hamada K, Shimizu T, Matsui T, Tsukita S, Hakoshima T. Structural basis of the membrane-targeting and unmasking mechanisms of the radixin FERM domain. EMBO J. 2000; 19:4449–4462. DOI: 10.1093/emboj/19.17.4449 [PubMed: 10970839]

Imada K, Leonard WJ. The Jak-STAT pathway. Molecular Immunology. 2000; 37:1–11. [PubMed: 10781830]

Lebrun JJ, Ali S, Ullrich A, Kelly PA. Proline-rich sequence-mediated Jak2 association to the prolactin receptor is required but not sufficient for signal transduction. J Biol Chem. 1995; 270:10664–10670. [PubMed: 7537736]

Leonard WJ, O'Shea JJ. Jaks and STATs: biological implications. Annu Rev Immunol. 1998; 16:293–322. DOI: 10.1146/annurev.immunol.16.1.293 [PubMed: 9597132]

Li Y, Li Y, Wei Z, Wei Z, Zhang J, Zhang J, Yang Z, Yang Z, Zhang M, Zhang M. Structural Basis of the Binding of Merlin FERM Domain to the E3 Ubiquitin Ligase Substrate Adaptor DCAF1. J Biol Chem. 2014; 289:14674–14681. DOI: 10.1074/jbc.M114.551184 [PubMed: 24706749]

Li Y, Zhou H, Li F, Chan SW, Lin Z, Wei Z, Yang Z, Guo F, Lim CJ, Xing W, Shen Y, Hong W, Long J, Zhang M. Angiomotin binding-induced activation of Merlin/NF2 in the Hippo pathway. Cell Res. 2015; 25:801–817. DOI: 10.1038/cr.2015.69 [PubMed: 26045165]

Lupardus PJ, Ultsch M, Wallweber H, Bir Kohli P, Johnson AR, Eigenbrot C. Structure of the pseudokinase-kinase domains from protein kinase TYK2 reveals a mechanism for Janus kinase (JAK) autoinhibition. Proc Natl Acad Sci USA. 2014; 111:8025–8030. DOI: 10.1073/pnas.1401180111 [PubMed: 24843152]

McNab F, Mayer-Barber K, Sher A, Wack A, O'Garra A. Type I interferons in infectious disease. Nat Rev Immunol. 2015; 15:87–103. DOI: 10.1038/nri3787 [PubMed: 25614319]

McNally R, Eck MJ. JAK–cytokine receptor recognition, unboxed. Nat Struct Mol Biol. 2014; 21:431–433. DOI: 10.1038/nsmb.2824 [PubMed: 24799036]

Murakami M, Narazaki M, Hibi M, Yawata H, Yasukawa K, Hamaguchi M, Taga T, Kishimoto T. Critical cytoplasmic region of the interleukin 6 signal transducer gp130 is conserved in the cytokine receptor family. Proc Natl Acad Sci USA. 1991; 88:11349–11353. [PubMed: 1662392]

Neubauer H, Cumano A, Müller M, Wu H, Huffstadt U, Pfeffer K. Jak2 deficiency defines an essential developmental checkpoint in definitive hematopoiesis. Cell. 1998; 93:397–409. [PubMed: 9590174]

Nicola NA, Hilton DJ. General classes and functions of four-helix bundle cytokines. Advances in protein chemistry. 1998; 52:1–65. [PubMed: 9917917]

O'Shea JJ, Schwartz DM, Villarino AV, Gadina M, McInnes IB, Laurence A. The JAK-STAT Pathway: Impact on Human Disease and Therapeutic Intervention*. Annu Rev Med. 2015; 66:311–328. DOI: 10.1146/annurev-med-051113-024537 [PubMed: 25587654]

Parganas E, Wang D, Stravopodis D, Topham DJ, Marine JC, Teglund S, Vanin EF, Bodner S, Colamonici OR, van Deursen JM, Grosveld G, Ihle JN. Jak2 is essential for signaling through a variety of cytokine receptors. Cell. 1998; 93:385–395. [PubMed: 9590173]

Pearson MA, Reczek D, Bretscher A, Karplus PA. Structure of the ERM protein moesin reveals the FERM domain fold masked by an extended actin binding tail domain. Cell. 2000; 101:259–270. [PubMed: 10847681]

Pelletier S, Pelletier S, Gingras S, Gingras S, Funakoshi-Tago M, Funakoshi-Tago M, Howell S, Howell S, Ihle JN, Ihle JN. Two Domains of the Erythropoietin Receptor Are Sufficient for Jak2 Binding/Activation and Function. Molecular and Cellular Biology. 2006; 26:8527–8538. DOI: 10.1128/MCB.01035-06 [PubMed: 16982687]

Pestka S, Krause CD, Walter MR. Interferons, interferon-like cytokines, and their receptors. Immunol Rev. 2004; 202:8–32. DOI: 10.1111/j.0105-2896.2004.00204.x [PubMed: 15546383]

Renauld JC. Class II cytokine receptors and their ligands: key antiviral and inflammatory modulators. Nat Rev Immunol. 2003; 3:667–676. DOI: 10.1038/nri1153 [PubMed: 12974481]

Rodig SJ, Meraz MA, White JM, Lampe PA, Riley JK, Arthur CD, King KL, Sheehan KC, Yin L, Pennica D, Johnson EM, Schreiber RD. Disruption of the Jak1 gene demonstrates obligatory and nonredundant roles of the Jaks in cytokine-induced biologic responses. Cell. 1998; 93:373–383. [PubMed: 9590172]

Royer Y, Royer Y, Staerk J, Staerk J, Costuleanu M, Costuleanu M, Courtoy PJ, Courtoy PJ, Constantinescu SN, Constantinescu SN. Janus Kinases Affect Thrombopoietin Receptor Cell Surface Localization and Stability. J Biol Chem. 2005; 280:27251–27261. DOI: 10.1074/jbc.M501376200 [PubMed: 15899890]

Schoenborn, JR.; Wilson, CB. Advances in Immunology. Elsevier; 2007. Regulation of Interferon- γ During Innate and Adaptive Immune Responses; p. 41-101.

Shan Y, Gnanasambandan K, Ungureanu D, Kim ET, Hammarén H, Yamashita K, Silvennoinen O, Shaw DE, Hubbard SR. Molecular basis for pseudokinase-dependent autoinhibition of JAK2 tyrosine kinase. Nat Struct Mol Biol. 2014; 21:579–584. DOI: 10.1038/nsmb.2849 [PubMed: 24918548]

Tanner JW, Chen W, Young RL, Longmore GD, Shaw AS. The conserved box 1 motif of cytokine receptors is required for association with JAK kinases. J Biol Chem. 1995; 270:6523–6530. [PubMed: 7896787]

Ungureanu D, Wu J, Pekkala T, Niranjan Y, Young C, Jensen ON, Xu CF, Neubert TA, Skoda RC, Hubbard SR, Silvennoinen O. The pseudokinase domain of JAK2 is a dual-specificity protein kinase that negatively regulates cytokine signaling. Nat Struct Mol Biol. 2011; 18:971–976. DOI: 10.1038/nsmb.2099 [PubMed: 21841788]

Usacheva A, Sandoval R, Domanski P, Kotenko SV, Nelms K, Goldsmith MA, Colamonici OR. Contribution of the Box 1 and Box 2 motifs of cytokine receptors to Jak1 association and activation. J Biol Chem. 2002; 277:48220–48226. DOI: 10.1074/jbc.M205757200 [PubMed: 12374810]

Wack A, Terczyńska-Dyla E, Hartmann R. Guarding the frontiers: the biology of type III interferons. Nat Immunol. 2015; 16:802–809. DOI: 10.1038/ni.3212 [PubMed: 26194286]

Wallweber HJA, Tam C, Franke Y, Starovasnik MA, Lupardus PJ. Structural basis of recognition of interferon-α receptor by tyrosine kinase 2. Nat Struct Mol Biol. 2014; 21:443–448. DOI: 10.1038/nsmb.2807 [PubMed: 24704786]

Wei Z, Li Y, Ye F, Zhang M. Structural Basis for the Phosphorylation-regulated Interaction between the Cytoplasmic Tail of Cell Polarity Protein Crumbs and the Actin-binding Protein *Moesin*. J Biol Chem. 2015; 290:11384–11392. DOI: 10.1074/jbc.M115.643791 [PubMed: 25792740]

Yan H, Piazza F, Krishnan K, Pine R, Krolewski JJ. Definition of the interferon-alpha receptor-binding domain on the TYK2 kinase. J Biol Chem. 1998; 273:4046–4051. [PubMed: 9461596]

Zhu MH, Berry JA, Russell SM, Leonard WJ. Delineation of the regions of interleukin-2 (IL-2) receptor beta chain important for association of Jak1 and Jak3. Jak1-independent functional recruitment of Jak3 to Il-2Rbeta. J Biol Chem. 1998; 273:10719–10725. [PubMed: 9553136]

HIGHLIGHTS

- IFNLR1 box1 and box2 motifs are required for stable complex formation with JAK1.
- Crystal structure of JAK1 reveals IFNLR1 box1-binding site in the FERM domain.
- Structure-based mutagenesis reveals IFNLR1 PxxLxF motif is essential for binding.
- Structure of JAK1 with IL10RA box1 indicates conservation among Class II receptors.

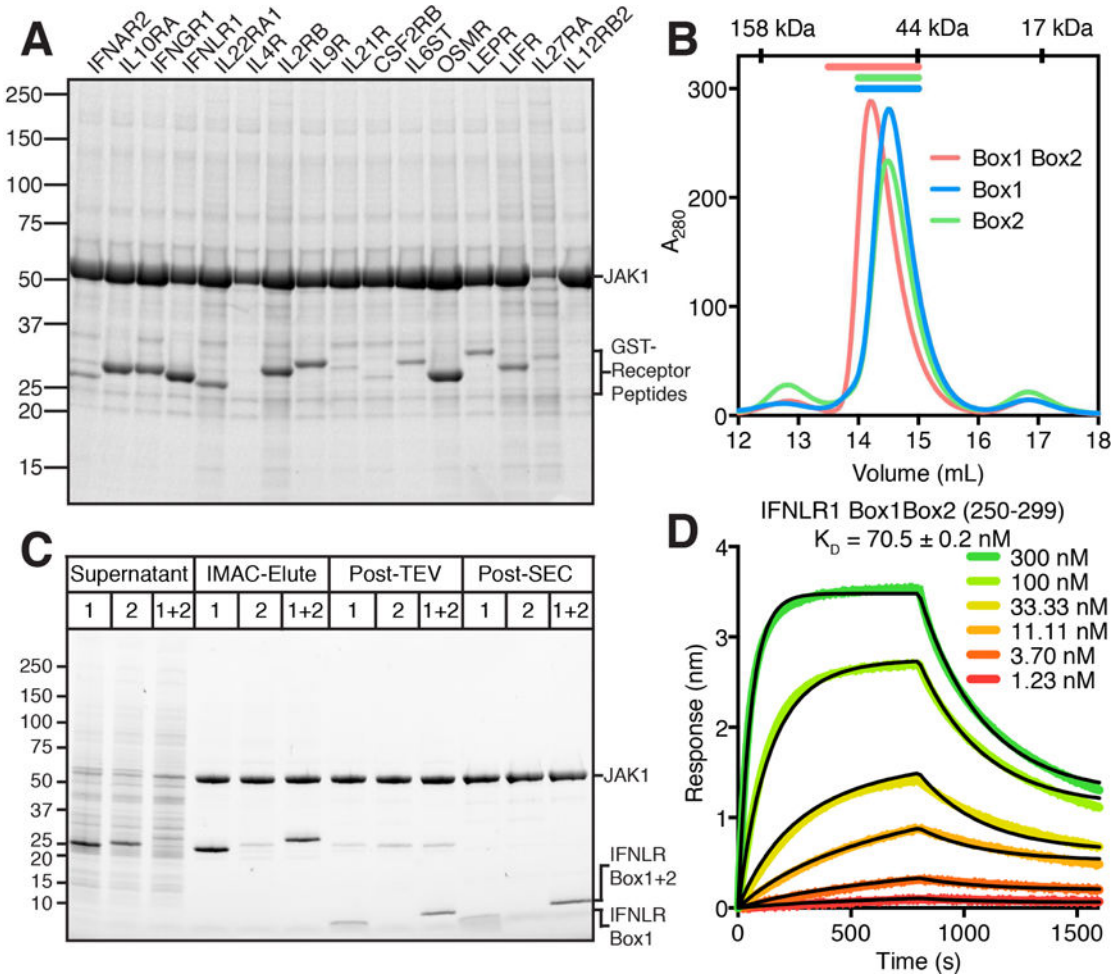

Figure 1. Identification and Characterization of a Stable JAK1–Receptor Peptide Complex

(A) SDS-PAGE analysis of His-JAK1 FERM–SH2 and GST-receptor peptide coexpressions after Ni-IMAC pull-down assay. Molecular weight markers indicated on left.

(B) SEC profiles of JAK1 coexpressed with IFNLR1 peptides containing box1 (residues 250–270, blue), box2 (residues 270–299, green), or both box1 and box2 (residues 250–299, red) binding sites. Size-exclusion standards are indicated at the top of the figure.

(C) SDS-PAGE analysis of His-JAK1 coexpressed with GST-IFNLR1 peptides containing box1, box2, or both box1 and box2 binding sites. Horizontal bars in (B) indicate fractions pooled for post-SEC lanes.

(D) BioLayer interferometry analysis of JAK1 binding to IFNLR1. Increasing concentrations of JAK1 were incubated with biotinylated IFNLR1 peptides containing both box1 and box2 motifs (residues 250–299) immobilized on a streptavidin biosensor. Assays were performed in triplicate, and the averaged data (various colors) were fit to a 1:1 binding model (black curves).

See also Figures S1 and S2.

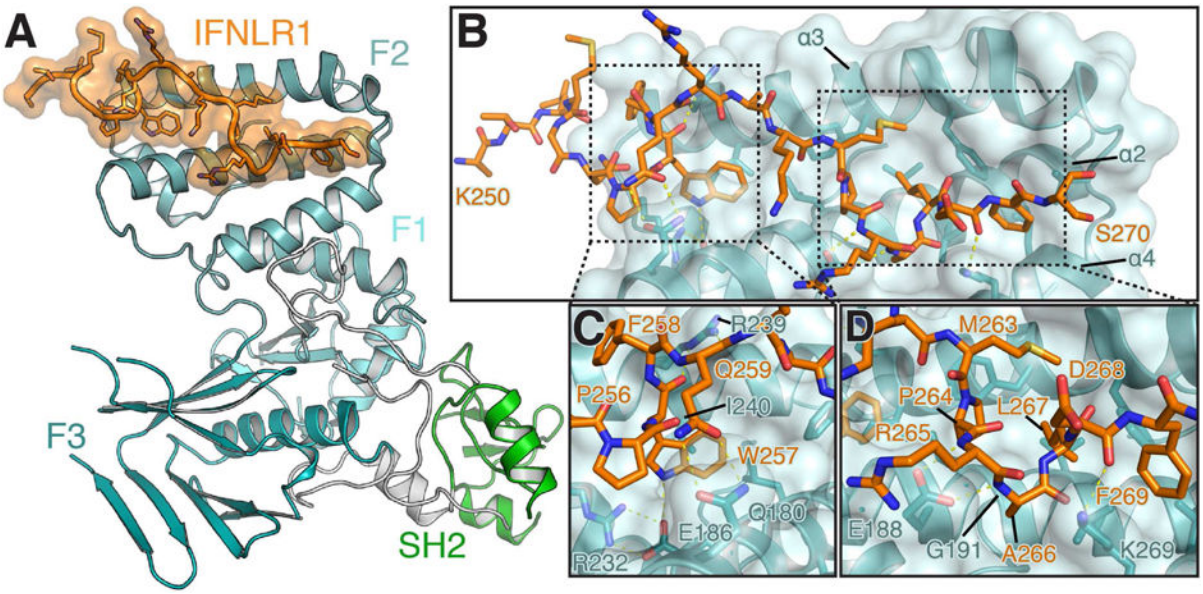

Figure 2. Structure of the JAK1 FERM–SH2 Domain Bound to the Box1 Site of IFNLR1

(A) Cartoon representation of the JAK1 FERM–SH2 (F1, F2, and F3, subdomains labeled and colored in shades of cyan, SH2 domain colored green) bound to IFNLR1 (orange, surface shown). Linkers between subdomains are colored grey.

(B) Overview of IFNLR1 peptide bound to the JAK1 F2 subdomain (surface shown). Key IFNLR1 and JAK1 residues are labeled and shown as sticks.

(C and D) The IFNLR1–JAK1 interface is further divided into the PWF interface, detailed in (C) and the PRALDF interface, detailed in (D).

See also Figures S3 and S4.

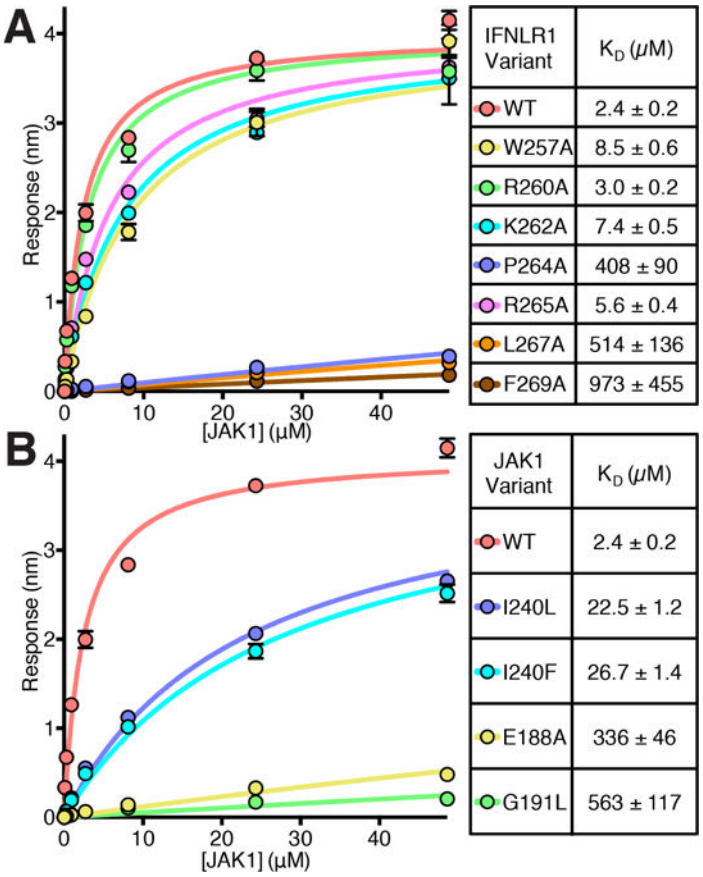

Figure 3. Identification of Key IFNLR1 Residues Essential for Binding to JAK1

(A) BioLayer Interferometry (BLI) was used to calculate steady state affinity (K_D) values for the interaction of JAK1 with biotinylated IFNLR1 peptides (residues 250–270) that contained alanine substitutions at key positions.

(B) As in (A), BLI was used to analyze binding of JAK1 mutants predicted to disrupt interaction with wild type IFNLR1.

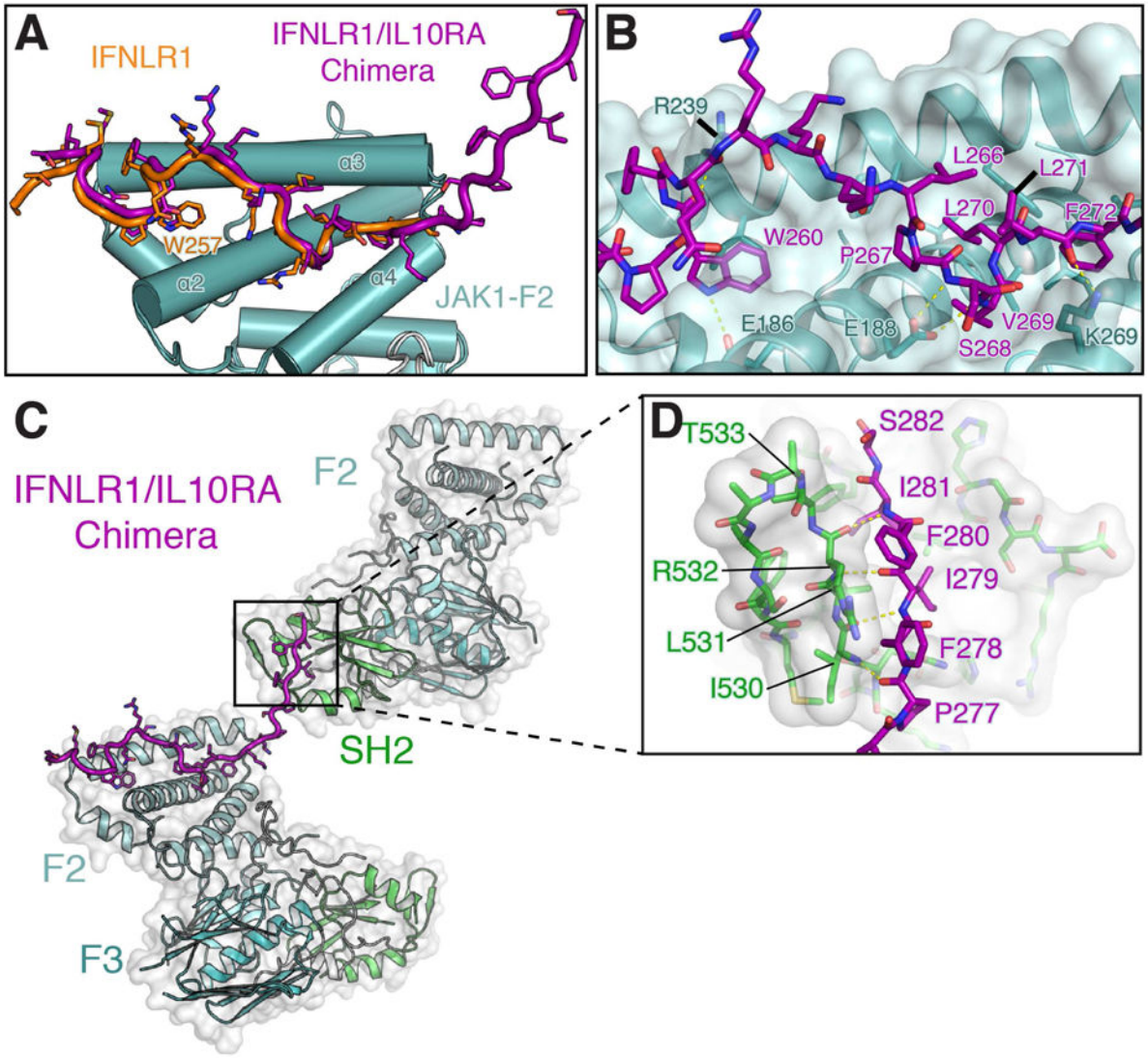

Figure 4. Structure of the IFNLR1–IL10RA Chimeric Receptor Bound to JAK1

(A) Overview of the IFNLR1–IL10RA chimera (purple) and IFNLR1 (orange) bound to the JAK1 FERM F2 domain (teal). Receptor backbone is displayed as a cartoon, with sidechains shown as sticks. Structural alignment is based on JAK1 FERM–SH2.

(B) Detailed interactions between JAK1 and the IFNLR1–IL10RA chimera. The receptor is shown as sticks, with JAK1 shown as a cartoon model with surface overlaid.

(C) A symmetry-related JAK1 molecule is displayed to show how IL10RA residues C-terminal to the box1 motif cross over from the FERM domain (cyan) of one JAK1 monomer to the SH2 domain (green) of a neighboring JAK1 monomer.

(D) Interactions between IL10RA residues Pro277-Ser282 bound to the neighboring JAK1 SH2 domain are detailed.

See also Figure S5.

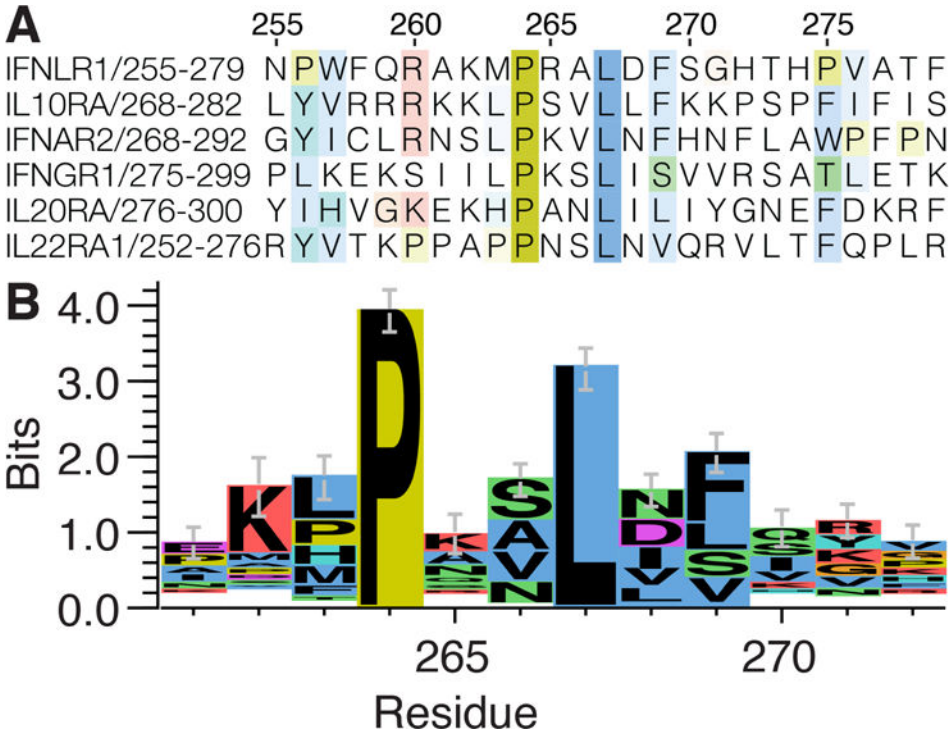

Figure 5. Residues Essential for the IFNLR1–JAK1 Interaction are Conserved among Class II Cytokine Receptors

(A) Multiple sequence alignment of the box1 motif of human class II cytokine receptors. Residues are colored in the ClustalX scheme with deepening color intensity indicating higher conservation. Numbering is based on IFNLR1 sequence.

(B) Sequence logo plot generated from an alignment of class II cytokine receptors from a broad group of higher eukaryotes. Sequences used for the analysis are detailed in the Methods section.

See also Figure S6.

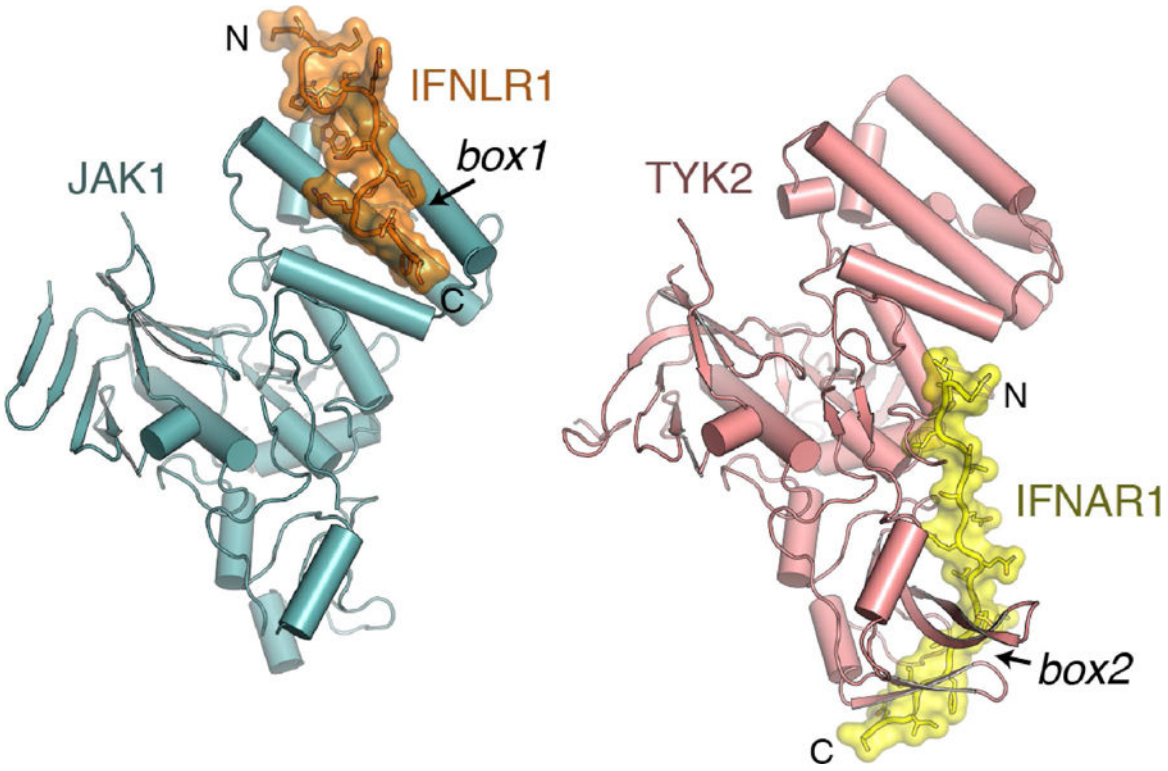

Figure 6. JAKs Interact with Receptor Box1 and Box2 Motifs via Distinct Binding Sites

JAK1 (teal) bound to the IFNLR1 box1 motif (orange) is shown on the left, and TYK2 (pink) bound to the type II cytokine receptor IFNAR1 box2 motif (yellow) is shown on the right. The Box1 interaction is mediated by the FERM F2 subdomain and box2 binding is primarily mediated by the SH2 domain.

See also Figure S7.

Table 1

Data Collection and Refinement Statistics.

	JAK1-IFNLR1 Native	JAK1-IFNLR1 Se-Met	JAK1-IFNLR1/10RA Native
Data collection			
Wavelength	0.9795	0.9794	1.0000
Space group	C 2 2 2_1	C 2 2 2_1	C2
Cell dimensions			
a, *b*, *c* (Å)	111.2, 193.2, 73.0	111.9, 195.1, 73.2	81.2, 110.4, 94.9
α, β, γ (°)	90, 90, 90	90, 90, 90	90, 98.1, 90
Resolution (Å)	44.29−.85 (2.95−2.85)	44.59−3.01 (3.12−3.01)	36.15−2.57 (2.66−2.57)
R_{merge}	0.055 (0.829)	0.069 (0.894)	0.083 (0.732)
$I/\sigma I$	20.1 (2.3)	31.2 (2.9)	13.8 (2.2)
Completeness (%)	99.4 (99.3)	99.2 (98.2)	99.4 (98.0)
Redundancy	5.1 (5.2)	13.3 (13.1)	3.7 (3.8)
Refinement			
Resolution (Å)	44.29−2.85	44.59−3.01	36.15−2.57
No. reflections	94781	215679	99064
R_{work}/R_{free} (%)	24.9/28.2	25.6/28.6	21.3/25.5
No. atoms			
Protein	3453	3480	3759
Water	0	0	69
B-factors			
Protein	97.35	112.40	63.68
Water			51.12
R.m.s. deviations			
Bond lengths (Å)	0.006	0.003	0.006
Bond angles (°)	1.04	0.69	1.01

* Values in parentheses are for highest-resolution shell.

Table 2

BioLayer Interferometry Kinetic Results

IFNLR1 peptide	K_D [95% confidence interval]	k_a ($M^{-1}s^{-1}$) [95% confidence interval]	k_d (s^{-1}) [95% confidence interval]
Box1Box2 (250–289)	70.5 ± 0.2 nM [70.1 to 70.8]	(5.04 ± 0.08) × 10^4 [5.03 to 5.06]	(3.55 ± 0.01) × 10^{-3} [3.54 to 3.57]
Box1 (250–270)	1.23 ± 0.01 μM [1.22 to 1.24]	(7.25 ± 0.05) × 10^4 [7.14 to 7.36]	(8.90 ± 0.06) × 10^{-2} [8.78 to 9.02]
Box1ΔBox2 (250–289)	1.57 ± 0.01 μM [1.56 to 1.59]	(3.46 ± 0.02) × 10^4 [3.42 to 3.50]	(5.44 ± 0.03) × 10^{-2} [5.38 to 5.49]

Note: The value range in parentheses are the 95% confidence limits associated with the parameter value returned and provide a measure of confidence in the model fit.